Modification of the nonlinear optical absorption and optical Kerr response exhibited by nc-Si embedded in a silicon-nitride film

A. López-Suárez[1*], C. Torres-Torres[2], R. Rangel-Rojo[3], J. A. Reyes-Esqueda[1], G. Santana[4], J. C. Alonso[4], A. Ortiz[4] and A. Oliver[1]

[1]*Instituto de Física, Universidad Nacional Autónoma de México, A.P. 20-364, México, D. F. 01000, México.*
[2]*Sección de Estudios de Posgrado e Investigación-ESIME-IPN, Zacatenco, México, D.F., 07738, México*
[3]*Department of Optics, Centro de Investigación Científica y de Educación Superior de Ensenada, A.P. 360, Ensenada, B.C. 22860 México*
[4]*Instituto de Investigaciones en Materiales. Universidad Nacional Autónoma de México, A.P. 70-360, México, D. F. 04510, México.*
[*]*Corresponding author: chipi72@gmail.com*

Abstract: We studied the absorptive and refractive nonlinearities at 532 nm and 26 ps pulses for silicon-nitride films containing silicon nanoclusters (nc-Si) prepared by remote plasma-enhanced chemical vapor deposition (RPECVD). Using a self-diffraction technique, we measured for the as-grown sample $\beta=7.7\times10^{-9}$m/W, $n_2=1.8\times10^{-16}$m^2/W, and $\left|\chi^{(3)}_{1111}\right|=4.6\times10^{-10}$esu; meanwhile, when the sample was exposed to an annealing process at 1000°C during one hour in a nitrogen atmosphere, we obtained $\beta=-5\times10^{-10}$m/W, $n_2=9\times10^{-17}$m^2/W, and $\left|\chi^{(3)}_{1111}\right|=1.1\times10^{-10}$esu. A pure electronic nonlinear refraction was identified and a large threshold ablation of 41 J/cm^2 was found for our films. By fitting nonlinear optical transmittance measurements, we were able to estimate that the annealed sample exhibits a response time close to 1 fs. We report an enhancement in the photoluminescence (PL) signal after the annealing process, as well as a red-shift due to an increment in size of the nc-Si during the thermal process.

OCIS codes: (160.4330) Nonlinear optical materials; (190.3270) Kerr effect; (160.4236) Nanomaterials.

References and links

1. T. Y. Kim, N.-M. Park, K.-H. Kim, G. Y. Sung, Y.-W. Ok, T.-Y. Sung, and C.-. Choi, "Quantum confinement effect of silicon nanocrystals in situ grown in silicon nitride films," Appl. Phys. Lett. **85**, 5355-5357. (2004).
2. T.-W. Kim, N. Park, K.-H. Kim, and G. Y. Sung, "Quantum confinement effect in crystalline silicon quantum dots in silicon nitride grown using SiH_4 and NH_3," Appl. Phys. Lett. **88**, 123102-123103 (2006).
3. N. Lalic and J. Linnros, "Light emitting diode structure based on Si nanocrystals by implantation into thermal oxide," J. Lumin. **80**, 263-267 (1999).
4. S.-H. Choi and R. G. Elliman, "Reversible charging effects in SiO_2 films containing silicon nanoparticles," Appl. Phys. Lett. **75**, 968-970 (1999).
5. D. J. Lockwood, Ed., *Light Emission in Silicon: From Physics to Devices*, (Academic, San Diego, 1998), Chap. 1.
6. J. S. Biteen, A. L. Tchebotareva, A. Polman, N. S. Lewis, and H. A. Atwater, "Controlled passivation and luminescence blue shifts of isolated silicon nancrystals," Mater. Res. Soc. Symp. Proc. **770**, I6.2.1 (2003).
7. A. Puzder, A. J. Williamson, J. C. Grossman, and G. Galli, "Surface chemistry of silicon nanoclusters," Phys. Rev. Lett. **88**, 097401-097401-4 (2002).
8. M. V. Wolkin, J. Jorne, P. M. Fauchet, G. Allan, and C. Delerue, "Electronic states and luminescence in porous silicon quantum dots: the role of oxygen," Phys. Rev. Lett. **82**, 197-200 (1999).
9. R.W. Boyd, *Nonlinear Optics*, (Academic Press, San Diego 1992).

#105953 - $15.00 USD Received 5 Jan 2009; revised 18 Mar 2009; accepted 25 Mar 2009; published 1 Jun 2009

10. Y. Li, S. Zhang, J. Liu, and K. Zhang, "Quantum correlation between fundamental and second-harmonic field via second-harmonic generation," J. Opt. Soc. Am. B **24**, 660-663 (2007).
11. M. D. Eisaman, A. Andra, F. Massou, M. Fleischhauer, A. S. Zibrov, and M. D. Lukin, "Electromagnetically induced transparency with tunable single-photon pulses," Nature **438**, 837-841 (2005).
12. J. P. Dowling, "Quantum information: To compute or not to compute?" Nature **439**, 919-920 (2006).
13. K. Ikeda, R. E. Saperstein, N. Alic, and Y. Fainman "Thermal on Kerr non linear properties of plasma-deposited silicon nitride/silicon dioxide waveguides," Opt. Express **16**, 12987-12994 (2008).
14. H. K. Tsang, C. S. Wong, T. K. Liang, I. E. Day, S. W. Roberts, A. Harpin, J. Drake, and M. Asghari, "Optical dispersion two-photon absorption and self-phase modulation in silicon waveguides at 1.5 μm wavelength," Appl. Phys. Lett. **80**, 416-418 (2002).
15. M. Dinu, F. Quochi, and H. Garcia, "Third-order nonlinearities in silicon at telecom wavelengths," Appl. Phys. Lett. **82**, 2954-2956 (2003).
16. T. Liang, L. Nunes, T. Sakamoto, K. Sasagawa, T. Kawanishi, M. Tsuchiya, G. Priem, D. Van Thourhout, P. Dumon, R. Baets, and H. Tsang, "Ultrafast all-optical switching by cross-absorption modulation in silicon wire waveguides," Opt. Express **13**, 7298-7303 (2005).
17. R. A. Soref and B. R. Bennett, "Electrooptical effects in silicon," IEEE J. Quantum Electron. **23**, 123-129 (1987).
18. V. R. Almeida, C. A. Barrios, R. R. Panepucci, and M. Lipson, "All-optical control of light on a silicon chip," Nature **431**, 1081-1084 (2004).
19. R. Claps, D. Dimitropoulos, Y. Han, and B. Jalali, "Observation of Raman emission in silicon waveguides at 1.54 μm," Opt. Express **10**, 1305-1313 (2002).
20. R. Claps, D. Dimitropoulos, and B. Jalali, "Stimulated Raman scattering in silicon waveguides," IEEE Electron. Lett. **38**, 1352-1354 (2002).
21. R. Claps, D. Dimitropoulos, V. Raghunathan, Y. Han, and B. Jalali, "Observation of stimulated Raman amplification in silicon waveguides," Opt. Express **11**, 1731-1739 (2003).
22. R. Jones, H. Rong, A. Liu, A. Fang, M. Paniccia, D. Hak, and O. Cohen, "Net continuous wave optical gain in a low loss silicon-on-insulator waveguide by stimulated Raman scattering," Opt. Express **13**, 519-525 (2005).
23. H. Rong, A. Liu, R. Jones, O. Cohen, D. Hak, R. Nicolaescu, A. Fang, and M. Panniccia, "An all-silicon Raman laser," Nature **433**, 292-294 (2005).
24. H. Rong, R. Jones, A. Liu, O. Cohen, D. Hak, A. Fang, and M. Paniccia, "A continuous-wave Raman silicon laser," Nature **433**, 725-728, (2005).
25. Y. Okawachi, M. Foster, J. Sharping, A. Gaeta, Q. Xu, and M. Lipson, "All-optical slow-light on a photonic chip," Opt. Express **14**, 2317-2322 (2006).
26. O. Boyraz, T. Indukuri, and B. Jalali, "Self-phase-modulation induced spectral broadening in silicon waveguides," Opt. Express **12**, 829-834 (2004).
27. A. Cowan, G. Rieger, and J. Young, "Nonlinear transmission of 1.5 mm pulses through single-mode silicon-on-insulator waveguide structures," Opt. Express **12**, 1611-1621 (2004).
28. O. Boyraz, P. Koonath, V. Raghunathan, and B. Jalali, "All-optical switching and continuum generation in silicon waveguides," Opt. Express **12**, 4094-4102 (2004).
29. J. E. Sharping, K. F. Lee, M. A. Foster, A. C. Turner, B. S. Schmidt, M. Lipson, A. L. Gaeta, and P. Kumar, "Generation of correlated photons in nanoscale silicon waveguides," Opt. Express **14**, 12388-12393 (2006).
30. M.A. Foster, A. C. Turner, R. Salem, M. Lipson, and A. L. Gaeta, "Broad-band continuous-wave parametric wavelength conversion in silicon waveguides," Opt. Express **15**, 12949-12958 (2007).
31. P. Cheng, H. Zhu, Y. Bai, Y. Zhang, T. He, and Y. Mo, "Third-order nonlinear optical response of silicon nanostructures dispersed in organic solvent under 1064 nm and 532 nm laser excitations," Opt. Commun. **270**, 391-395 (2007).
32. H. Yıldırım and C. Bulutay, "Enhancement of optical switching parameter and third-order optical nonlinearities in embedded Si nanocrystals: a theoretical assessment," Opt. Commun. **281**, 4118-4120 (2008).
33. E. Koudoumas, O. Kokkinaki, M. Konstantaki, N. Kornilios, S. Couris, S. Korovin, V. Pustovoi, and V. E. Ogluzdin, "Nonlinear optical response of silicon nanocrystals," Opt. Mater. **30**, 260-263 (2007).
34. H. S. Mavi, S. Prusty, A. K. Shukla, and S. C. Abbi, "Nonlinear phenomenon in nanocrystallites produced by laser-induced etching of silicon," Opt. Commun. **226**, 405-413 (2003).
35. S. Hernández, P. Pellegrino, A. Martínez, Y. Lebour, B. Garrido, R. Spano, M. Cazzanelli, N. Daldosso, L. Pavesi, E. Jordana, and J. M. Fedeli, "Linear and nonlinear optical properties of Si nanocrystals in SiO_2 deposited by plasma-enhanced chemical-vapor deposition," J. Appl. Phys. **103**, 064309- 064309-6 (2008).
36. C. Torres-Torres, A. López-Suárez, L. Tamayo-Rivera, R. Rangel-Rojo, A. Crespo-Sosa, J .C. Alonso, and A. Oliver, "Thermo-optic effect and optical third order nonlinearity in nc-Si embedded in a silicon nitride film," Opt. Express, **16**, 18390-18396 (2008)
37. M. Mayer, *SIMNRA User's Guide*, Version 6.0, (Max Planck-Institute für Plasmaphysik, Garching).

#105953 - $15.00 USD Received 5 Jan 2009; revised 18 Mar 2009; accepted 25 Mar 2009; published 1 Jun 2009

38. C. Torres-Torres, A. V. Khomenko, J. C. Cheang-Wong, L. Rodríguez-Fernández, A. Crespo-Sosa, and A. Oliver, "Absorptive and refractive nonlinearities by four-wave mixing for Au nanoparticles in ion-implanted silica," Opt. Express **15**, 9248-9253 (2007).
39. G. Santana, B. M. Monroy, A. Ortiz, L. Huerta, J. C. Alonso, J. Fandiño, J. Aguilar-Hernández, E. Hoyos, F Cruz-Gandarilla, and G. Contreras-Puentes, "Influence of the surrounding host in obtaining tunable and strong visible photoluminescence from silicon nanoparticles," Appl. Phys. Lett. **88**, 041916-041916-3 (2006).
40. A. López-Suárez, J. Fandiño, G. Santana, and J. C. Alonso, "Study of the influence of NH_3 flow rates on the structure and photoluminescence of silicon-nitride films with silicon nanoparticles," Physica E **40**, 3141-3146 (2008).
41. V. B.-H. Kim, K.-H. Kim, C.-H. Cho, T.-W. Kim, N.-M. Park, G. Y. Sung, and S.-J. Park, "Photoluminescence of silicon quantum dots in silicon nitride grown by NH_3 and SiH_4," APL **86**, 091908-091908-3 (2005).
42. K. S. Min, K. V. Shcheglov, C. M. Yang, H. A. Atwater, M. L. Brongersma, and A. Polman, "Defect related versus excitonic visible light emission from ion beam synthesized Si nanocrystals in SiO_2," Appl. Phys. Lett. **69**, 2033-2035 (1996).
43. S. P. Withrow, C. W. White, A. Meldrum, J. D. Budai, D. M. Hembree, Jr., and J. C. Barbour, "Effects of hydrogen in the annealing environment on photoluminescence from Si nanoparticles in SiO_2," J. Appl. Phys. **86**, 396-401 (1999).
44. C. Torres-Torres and A. V. Khomenko, "Autodifracción vectorial de dos ondas degeneradas en medios con efecto Kerr óptico," Revista Mexicana de Física. **51**,162-167 (2005).
45. M. Sheik-Bahae, D. C. Hutchings, D. J. Hagan, E. W. Van Stryland, "Dispersion of bound electron nonlinear refraction in solids," IEEE J. Quantum Electron. **27**, 1296-1309 (1991).
46. M. Sheik-Bahae, A. A. Said, Tahi-Huei Wei, D. J. Hagan, E. W. Van Stryland, "Sensitive measurement of optical nonlinearities using a single beam," IEEE J. Quantum Electron. **17-26**, 760 (1990).
47. G. Heng-Qun and W. Qi-Ming, "Nonlinear Optical Response of nc-Si-SiO2 Films Studied with Femtosecond Four-Wave Mixing Technique," Chin. Phys. Lett., **23**, 2989-2992, (2006).
48. P. Zhou, G. You, J. Li, S. Wang, S. Qian, and L. Chen "Annealing effect of linear and nonlinear optical properties of Ag:Bi_2O_3 nanocomposite films," Opt. Express. **13**, 1508-1514 (2005).
49. R. Rangel-Rojo, K. Kimura, H. Matsuda, M. A. Mendez-Rojas, and W. H. Watson, "Dispersion of the third-order nonlinearity of a metallo-organic compound," Opt. Commun. **228**, 181-186 (2003).

1. Introduction

Lately, the ability of forming silicon-based low-dimensional structures, such as quantum-dots, has drawn much attention into the possibility of fabricating nano-optoelectronic devices [1-4]. This interest is due to the fact that silicon nanostructures posses optical and electrical properties quite different from those of bulk silicon. In particular, silicon nanoparticles show a quantum confinement effect, which causes an enhanced rate of radiative recombination of excitons [5]. In this direction, the choice of the matrix containing the silicon nanoparticles is quite important, since it has been observed that nc-Si grown in a silicon oxide matrix may not present PL associated to such a quantum confinement effect [6,7], due to the presence of silicon-oxide double bonds, which may produce localized levels in the band-gap of the nc-Si, as proposed by Wolkin et al. [8] On the contrary, a silicon-nitride matrix containing nanoparticles has been found to provide a good PL emission, demonstrating potential for fabrication of light-emitting diodes (LEDs) at very low cost in a wide range of luminescent wavelengths, just by controlling the nc-Si size [1].

On the other hand, there is also a great interest in developing new nonlinear optical materials for a great variety of applications, for instance in optics communication [9] or in the fast growing field of quantum information [10-12]. In this direction, nonlinear optical effects such as the Kerr effect have been demonstrated in silicon nitride [13]; while two-photon absorption [14-16] (TPA), free-carrier dispersion [17,18], Raman effect [19-25], Kerr effect [14,15,26-29], and broad-band continuous-wave parametric wavelength conversion for waveguides [30], have all been demonstrated in silicon. In particular, for optoelectronic nanodevices and all-optical switching with nc-Si, TPA and Kerr effect have been studied [30-35] finding that the electronic response is enhanced due to quantum confinement effects. Specifically, the electronic susceptibility, associated with intraband transitions, increases as the size of the nc-Si is reduced, due to the appearance of electronic transitions between discrete levels induced by quantum confinement [35]. For nc-Si embedded in a silicon-nitride

#105953 - $15.00 USD Received 5 Jan 2009; revised 18 Mar 2009; accepted 25 Mar 2009; published 1 Jun 2009

film, it has been demonstrated that the third order nonlinear response can be enhanced by the combination of different mechanisms of nonlinear refraction, specifically, electronic polarization and thermo-optic properties [36].

In this work, we use the RPECVD technique in order to grow silicon-nitride films on quartz substrates and we study their optical properties before and after a high temperature thermal annealing. We measure the PL signal of the samples, relating the position of the peaks to the size of the nc-Si by using a quantum confinement model for crystalline nanoparticles. Most importantly, when we measure the third-order nonlinear optical response at 532 nm in the picosecond regimen, we show that they can exhibit different mechanisms of nonlinear absorption.

2. Experiment

The silicon-nitride films were prepared using a RPECVD system. The films were grown on quartz substrates using a working pressure of 300 mTorr, a substrate temperature of 300°C and a rf power of 200 W. The flow rates of H_2, Ar, SiH_2Cl_2 and NH_3 were 20, 150, 5 and 50 sccm, respectively. During the deposition, Ar and NH_3 gases were fed from the top of the chamber where the plasma is generated; meanwhile, the H_2 and SiH_2Cl_2 gases were fed downstream the plasma zone by means of a dispersal ring located over the substrate holder. In order to increase the nc-Si density as well as to improve its PL signal, one of the samples was annealed in a N_2 atmosphere at 1000°C during 1 hour.

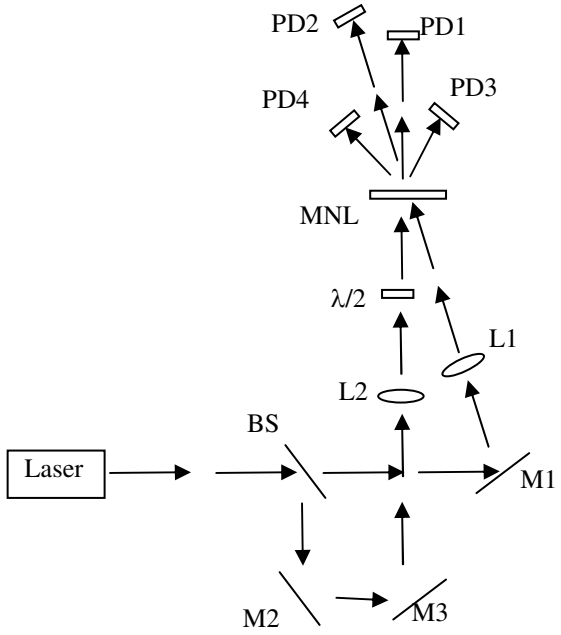

Fig. 1. Nonlinear optical experimental set up

Rutherford Backscattering Spectrometry (RBS) was used to determine the elemental composition of the films before and after annealing. A collimated 3.045 MeV α-particle beam with a 2 mm diameter, a 50 nA mean ion current, and a beam charge of 30 μC, was used to obtain the atomic concentration of the elements that formed the sample. This measurement was performed using the 3 MV Tandem accelerator (NEC 9SDH-2 Pelletron) facility at the Instituto de Física of the Universidad Nacional Autónoma de México. Projectiles that scattered at 167° were detected with a surface barrier detector. The simulation and analysis of RBS spectra were done with the SIMNRA code [37]. The film thickness was measured using

#105953 - $15.00 USD Received 5 Jan 2009; revised 18 Mar 2009; accepted 25 Mar 2009; published 1 Jun 2009

a profilometer system and was verified by RBS as the energy loss of the helium beam as it interacts with the electrons and atoms present in the sample.
PL experiments were carried out at room temperature in a conventional PL system. A 10 mW He-Cd laser (325 nm) was used as the excitation source. The silicon-nitride films were also characterized by High-Resolution Transmission Electronic Microscopy (HRTEM). The HRTEM studies were performed using a JEOL JEM-2010F microscope operating at 200 kV and equipped with a GATAN digital micrograph system for image acquisition.

In order to measure the nonlinear optical response, we used a self-diffraction technique [38] at 532nm and 26ps with linear polarization. The maximum pulse energy in our experiment was 0.2 mJ. The irradiance rate I_1:I_2 was 1:1. The radius of the beam waist at the focus in the sample was measured to be 0.15 mm. Fig. 1 shows the experimental set-up, where L1-2 represent the focusing system of lenses, BS is a beam splitter, λ/2 is a half-wave plate, M1-3 are mirrors, MNL is the sample, and PD1-4 are photodetectors.

3. Results and discussion

The RBS results showed the following atomic concentrations for both samples: 68% Si, 20% N and 12% Cl for the as-grown film and 60% Si, 18% N, 3% Cl and 19% O for the annealed sample. The RBS spectrum of the annealed sample is shown in Fig. 2, where the different steps are related to each element present in the film; meanwhile, the large peak corresponds to oxygen. In order to resolve this large oxygen peak, it was necessary to improve the sensitivity of the system. Typical RBS measurements are obtained at 2 MeV, but at this energy, the oxygen signal overlaps with the nitrogen signal and if oxygen concentration is small, it is almost impossible to visualize the element in the spectra. To avoid these problems, we increased the incident energy of the alpha particles used as projectiles up to 3.045 MeV, which corresponds to one of the oxygen resonance energies. These resonances are regions where the scattering cross section is greatly enhanced over the Rutherford cross section at the same energy, so elements with small concentrations can be measured.

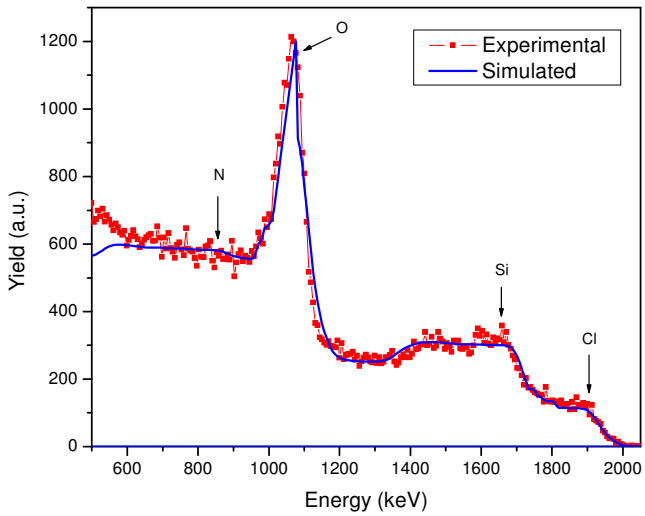

Fig. 2. RBS spectrum of the annealed film, where the elements present in the sample are shown. We took advantage of the elastic scattering resonance $^{16}O(\alpha,\alpha)^{16}O$ at 3.045 MeV, which is 25 times larger than its corresponding Rutherford cross section, in order to obtain high sensitivity in the oxygen measurement

The as-grown sample did not show any oxygen concentration, what made us think that both samples were chemically stable after they left the growing chamber and stayed at room

#105953 - $15.00 USD Received 5 Jan 2009; revised 18 Mar 2009; accepted 25 Mar 2009; published 1 Jun 2009

temperature. On the other hand, the large amount of oxygen detected in this RBS spectrum for the annealed film can be explained as follows. Films with large Cl concentration (as it was the case in our samples) tend to be porous and easily suffer a fast and complex hydroxilization/oxidation process. During the thermal treatment, the chlorine is removed from the films and it is substituted by oxygen atoms coming from the nitrogen gas that may contain oxygen impurities, as well as from the air when samples get exposed to the atmosphere during the annealing process [39]. This Cl substitution leads to the formation of non-stoichiometric silicon oxynitrides [40] with a reduced amount of Cl, as was verified through the RBS analysis.

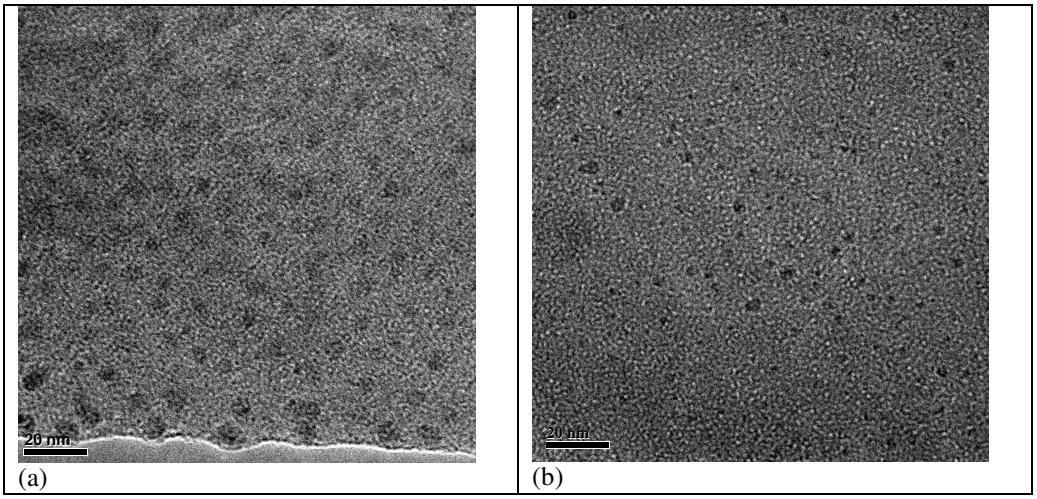

Fig. 3. (a) HRTEM micrograph of the silicon-nitride film after the annealed process. The small rounded dark spots correspond to nc-Si. (b) HRTEM micrograph of the as-grown sample.

Figure 3 shows the HRTEM micrographs of the samples, where several dark spots that correspond to nc-Si can be observed. A statistical analysis of the HRTEM micrographs in different zones of the samples was made in order to get the size distribution and the density of the nc-Si as precisely as possible. The results of this analysis showed that the nc-Si size in the as-grown sample varies in the range from 2.1 nm to 4.2 nm, with an average size of 3.2 nm and a density of approximately $(0.89\pm0.13)\times10^{11}cm^{-2}$; while in the annealed sample the nc-Si size varies in the range from 2.7 to 5.7 nm, with an average size of 4.5 nm and a density of approximately $(2.20\pm0.31)\times10^{11}cm^{-2}$. The difference in size and density of the nc-Si in both samples is a direct consequence of the annealing process. This thermal treatment, which gives energy to the system, contributes in particle formation and size increment in two different ways. The first uses energy to nucleate the silicon atoms present in the silicon-nitride film and form the silicon nanoparticles. On the other hand, nc-Si increase their size because energy tends to incorporate silicon atoms to the nc-Si previously formed during the RPECVD technique, or by coalescing together two or more nc-Si of small size to form a bigger nc-Si. In this way, the density as well as the size of the nc-Si increase. In order to obtain the composition of the nc-Si in both samples, an EDX measure was performed using the high resolution transmission microscope. The results showed the following elemental concentration. In the case of the as-grown film the nc-Si composition was 97% Si and 3% Cu, while for the annealed film the nc-Si were composed by 94% Si, 3% O and 3% Cu, respectively. This result showed that the annealing treatment tends to oxidize the whole film, including the nanoparticles embedded inside it. The Cu signal comes from the Cu gratings used to support the silicon-nitride films during the HRTEM analysis. The HRTEM micrographs showed the crystallographic planes of the nc-Si that were verified using the Fourier Transform (FT) analysis. According to these results, we can assure that the nanoparticles formed in the silicon-nitride film during the preparation using RPECVD

#105953 - $15.00 USD Received 5 Jan 2009; revised 18 Mar 2009; accepted 25 Mar 2009; published 1 Jun 2009

technique, as well as during the annealing process, are composed by silicon and are crystalline.

Figure 4 shows the PL spectra of the film before and after the annealing process. It can be observed that the PL signal increased after the annealing process as a consequence of the increment in the number of nc-Si per unit of volume. It is worth remarking that this increment was observed previously for samples annealed in N_2 atmosphere; however, most of the nc-Si in that case, was in the amorphous state [41]. The annealed film showed four peaks, two of them of significant intensity located at 1.60 eV and 1.92 eV, and two smaller ones at 2.52 eV and 2.88 eV, while the as-grown sample showed one well defined peak located at 2.19 eV and a smaller one at 2.85 eV. The PL in the films is produced by a quantum confinement effect due to the nc-Si embedded in the silicon-nitride matrix, as it has been observed by other authors [41], while the enhancement after the annealing process may be attributed to two processes. The first one, as was previously discussed, is due to the increment in the number of nc-Si during the thermal treatment as it was observed during the statistical HRTEM analysis; the second process can be attributed to defects produced by silicon and/or nitrogen dangling bonds [42,43].

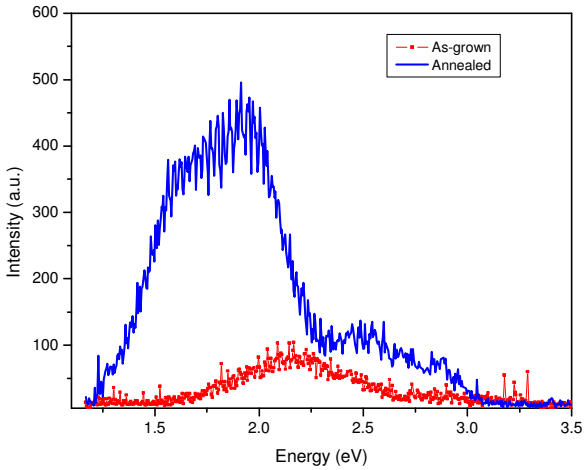

Fig. 4. PL spectrum of the silicon nitride films before (as-grown) and after the annealing treatment. An enhancement in the PL signal as well as a red-shift is observed after the annealing process.

Another fact that is in accordance to the quantum confinement theory is the red-shift of the PL peaks of the annealed sample that is observed in Fig. 4. Quantum confinement theory assumes that the nanoparticle acts as a box of infinite walls with energy $W_n = n^2h^2/8ma^2$, where a is the size of the box. As the size of the nanoparticle increases, the energy decreases and an increment in the associated wavelength can be observed. For this reason, an increase in the nc-Si size is related to a red-shift in the spectrum. The presence of multiple PL peaks means that the nc-Si are different in size. According to the quantum confinement model [1], the average size of the quantum dots or nanoclusters can be calculated using the relation for crystalline nc-Si, $W(\text{eV}) = W_{\text{bulk}} + C/a^2 = 1.16 + 11.8/a^2$, where W is the measured PL energy peak, W_{bulk} is the band-gap energy of the bulk crystal silicon, C is the quantum confinement parameter and a is the average size (nm) of the nanocluster. In our case, the calculated average sizes of the nc-Si are 5.2, 3.9, 2.9 and 2.6 nm, corresponding to the peaks located at 1.60, 1.92, 2.52 and 2.88 eV, respectively for the annealed sample. In the case of the as-grown film, the average sizes of the nc-Si are 3.3 and 2.6 nm, which correspond to energies values of 2.19 and 2.85 eV, respectively. We noticed a good agreement between the average sizes of the nc-Si measured from the HRTEM micrographs and the ones obtained using the quantum

#105953 - $15.00 USD Received 5 Jan 2009; revised 18 Mar 2009; accepted 25 Mar 2009; published 1 Jun 2009

confinement model for crystalline nc-Si. Since the density of the nc-Si is proportional to the height of the PL peaks, we would expect to have less nc-Si of smallest size as the peaks located at bigger energies are weaker than the ones located at smaller energies that correspond to stronger peaks.

The interaction of the two incident and the self-diffracted waves in nonlinear absorbing media can be described by [38],

$$E_{1\pm}(z)=\left[J_0\left(\Psi_{\pm}^{(1)}\right)E_{1\pm}^{0}+iJ_1\left(\Psi_{\pm}^{(1)}\right)E_{2\pm}^{0}\right]\exp\left(-i\Psi_{\pm}^{(0)}-\frac{\alpha(I)z}{2}\right), \tag{1}$$

$$E_{2\pm}(z)=\left[J_0\left(\Psi_{\pm}^{(1)}\right)E_{2\pm}^{0}-iJ_1\left(\Psi_{\pm}^{(1)}\right)E_{1\pm}^{0}\right]\exp\left(-i\Psi_{\pm}^{(0)}-\frac{\alpha(I)z}{2}\right), \tag{2}$$

$$E_{3\pm}(z)=\left[iJ_1\left(\Psi_{\pm}^{(1)}\right)E_{1\pm}^{0}-J_2\left(\Psi_{\pm}^{(1)}\right)E_{2\pm}^{0}\right]\exp\left(-i\Psi_{\pm}^{(0)}-\frac{\alpha(I)z}{2}\right), \tag{3}$$

$$E_{4\pm}(z)=\left[-iJ_1\left(\Psi_{\pm}^{(1)}\right)E_{2\pm}^{0}-J_2\left(\Psi_{\pm}^{(1)}\right)E_{1\pm}^{0}\right]\exp\left(-i\Psi_{\pm}^{(0)}-\frac{\alpha(I)z}{2}\right), \tag{4}$$

where $E_{1\pm}(z)$ and $E_{2\pm}(z)$ are the complex amplitudes of the circular components of the transmitted waves beams; $E_{3\pm}(z)$ and $E_{4\pm}(z)$ are the amplitudes of the self-diffracted waves; while $E_{1\pm}^{0}$ and $E_{2\pm}^{0}$ are the amplitudes of the incident waves; $\alpha(I)=\alpha_0+\beta I$, is the irradiance dependent absorption coefficient, α_0 and β are the linear and nonlinear absorption coefficient, I is the total irradiance of the incident beams, J_m ($\Psi_{\pm}^{(1)}$) stands for the Bessel function of order m, z is the thickness of the nonlinear media, and

$$\Psi_{\pm}^{(0)}=\frac{4\pi^2 z}{n_0\lambda}\left[A\left(\left|E_{1\pm}\right|^2+\left|E_{2\pm}\right|^2\right)+(A+B)\left(\left|E_{1\mp}\right|^2+\left|E_{2\mp}\right|^2\right)\right], \tag{5}$$

$$\Psi_{\pm}^{(1)}=\frac{4\pi^2 z}{n_0\lambda}\left[A\,E_{1\pm}E_{2\pm}^{*}+(A+B)\,E_{1\mp}E_{2\mp}^{*}\right], \tag{6}$$

are the phase increments when we consider that our material is isotropic and therefore $A=6\chi_{1122}^{(3)}=3\chi_{1122}^{(3)}+3\chi_{1212}^{(3)}$ and $B=6\chi_{1221}^{(3)}$.

Our measurement system was previously calibrated using CS_2 with a thickness D = 1 mm, as a nonlinear medium with a well known third-order nonlinear susceptibility of $\left|\chi^{(3)}\right|$ = 1.9×10^{-12} esu[9]. In our case, the annealed silicon-nitride sample has a thickness D = 1.76±0.18 μm, while for the as-grown sample D = 1.003±0.12 μm. With single pulses at λ=532 nm and 26 ps, we observed an ablation threshold in both films of 41 J/cm^2±10%. We guaranteed that there was not optical damage in either sample during the self-diffraction experiments by using fluences below this ablation threshold. The irradiances of the diffracted and transmitted beams behind the sample were measured when the incident waves $\vec{E}_1$ and $\vec{E}_2$ had parallel linear polarizations. An error bar of ±10% was estimated for the experimental irradiance data. We also obtained the irradiance of the self-diffracted wave $\vec{E}_3$ in the experiment, but in this case the polarization of the wave $\vec{E}_1$ was fixed while the polarization of the wave $\vec{E}_2$ was rotated by a half-wave plate λ/2.

From the ratio of maximum to minimum self-diffracted irradiances generated by the vectorial mixing of the two incident waves, the physical mechanism of nonlinear refraction

#105953 - $15.00 USD Received 5 Jan 2009; revised 18 Mar 2009; accepted 25 Mar 2009; published 1 Jun 2009

could be identified [44]. From Fig. 5, a nonzero self-diffracted irradiance can be observed for all the angles between the polarizations of the two waves. From our numerical simulations using Eqs. (1-4), and the experimental data shown in Fig. 5, we deduced that the *B/A* ratio can be approximated to the value *B/A*=1. This result allowed us to identify a pure electronic polarization as the physical mechanism responsible for nonlinear refraction in our samples, taking into account that nonlinear optical absorption was also present. This electronic response has been proposed to be associated to quantum confinement effects, which would induce the appearance of electronic transitions between discrete levels, increasing, in consequence, the electronic susceptibility [35].

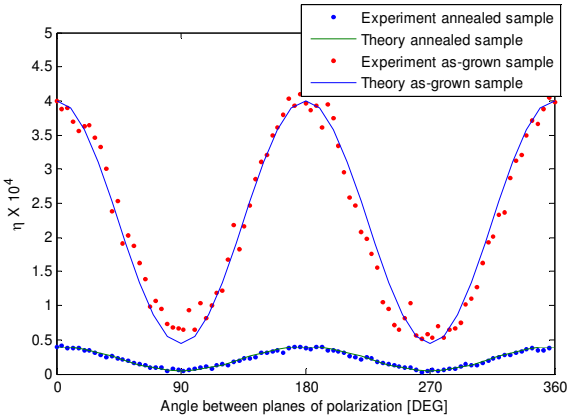

Fig. 5. Self-diffraction efficiency as a function of the angle ϕ between planes of polarization of the incident waves.

By comparing numerical simulations of Eqs. (1-6) with the data obtained from the self-diffracted and transmitted irradiances in CS_2 and that obtained from the nc-Si in both samples, we obtained for the annealed sample α_0=1.70273×10^5 m^{-1}, β=-5×10^{-10}m/W, n_2=9×10^{-17}m^2/W, and $\left|\chi^{(3)}_{1111}\right|$=1.1×10^{-10}esu; meanwhile, for the as-grown sample the corresponding values were α_0=4.04×10^5 m^{-1}, β=7.7×10^{-9}m/W, n_2=1.8×10^{-16}m^2/W, and $\left|\chi^{(3)}_{1111}\right|$ = 4.6×10^{-10}esu. By rotating simultaneously the polarization of the two incident waves in the experiment, we guaranteed that the optical absorption is completely isotropic. From these results, we conclude that the material presents nonlinear refraction that could be associated with an electronic mechanism, which has been enhanced due to quantum confinement effects [35]. A positive β value is consistent with the presence of either TPA, or induced absorption produced by strong excited-state absorption, while a negative β value is related with the presence of saturable absorption. Although saturable absorption is not strictly a third-order process, for small absorption changes it can be approximated as a third-order one[45], *i.e.* $\alpha=\alpha_0/(1+I/I_s)$, where I_s is the saturation irradiance. This expression can be approximated to $\alpha\approx\alpha_0-(\alpha_0/I_s)I$, and therefore,

$$\beta = -\frac{\alpha_o}{I_s}. \tag{7}$$

In order to further investigate the mechanism of nonlinear optical absorption, an input-output experiment was made in both samples. Fig. 6 and Fig. 7 shows the theoretical and experimental results for the transmittance of the samples as a function of the input irradiance; the fit of the data was obtained using the well known expression for the transmitted irradiance *I(z)* in the presence of nonlinear absorption[46]:

#105953 - $15.00 USD Received 5 Jan 2009; revised 18 Mar 2009; accepted 25 Mar 2009; published 1 Jun 2009

$$I(z) = \frac{I_0 \exp(-\alpha_o z)}{1 + \beta I_0 z}, \tag{8}$$

and the values of nonlinear absorption coefficients obtained with the self-diffraction measurements.

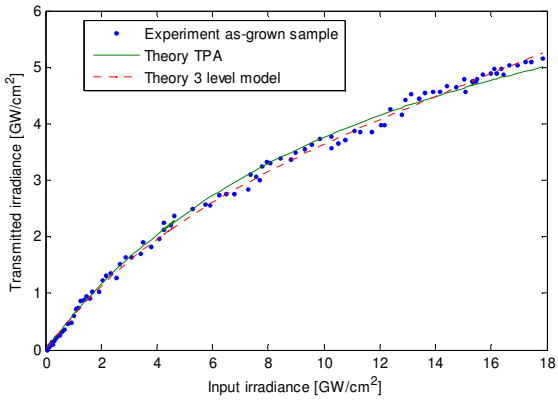

(a)

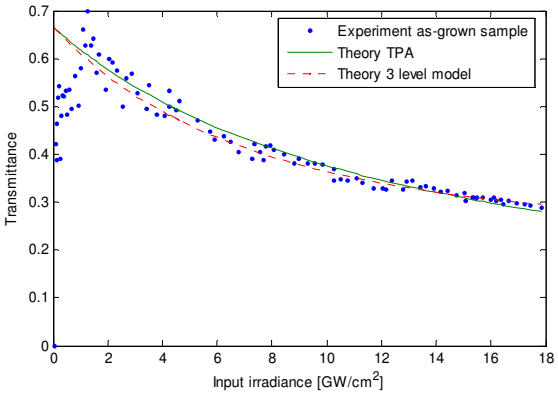

(b)

Fig. 6. Optical transmittance through the as-grown sample (a) transmitted vs. incident irradiance, (b) transmittance as function of incident irradiance.

The results presented in Fig. 6 and Fig. 7, confirm that different nonlinear absorption effects took place in the samples. The figures clearly show that the annealed sample presents saturable absorption, while the as-grown sample exhibits induced absorption.

The saturation irradiance for the annealed sample can be obtained substituting the value of α_0=1.70273×10^5 m^{-1} and β=-5×10^{-10}m/W in Eq. (7) that is consistent with the self-diffraction experiment and with the best fit made with Eq. (8) to the input-output experiment data; the resulting value is I_s=3.4055×10^{14} W/m^2.

For photon energies close to resonance with an electronic transition, it is possible to express I_s as,

$$I_s = \hbar\omega / \sigma\tau_0 \tag{9}$$

where $\hbar\omega$ is the photon energy, σ is the absorption cross-section of the transition and τ is the corresponding lifetime of the excited state. Similar samples have been studied experimentally with femtosecond pulses, but the response time of the nc-Si could not be identified [36,47]. At this point, the response time given by τ can be estimated in the annealed sample if we consider a two level model where,

$$\alpha_o = \sigma N_0, \tag{10}$$

#105953 - $15.00 USD Received 5 Jan 2009; revised 18 Mar 2009; accepted 25 Mar 2009; published 1 Jun 2009

where N_0 is the number density and α_0 is the measured value of the linear absorption coefficient. By means of our statistical data for the density of nc-Si, we approximate N_0=1.0319×10^{23} m^{-3} and then we use Eq. (10), the result is σ=1.6401×10^{-18}m^{-2}. Because in our case, $\hbar\omega$=3.7365×10^{-19} J, we substitute these values in Eq. (9), from where we estimate that the annealed sample exhibits a lifetime τ =7×10^{-16}*s*, *i.e.* close to *1 fs*. This is consistent with previous time-resolved Kerr effect experiments conducted with similar samples, which showed a response time shorter than the 80 fs pulse duration employed in the experiments [36].

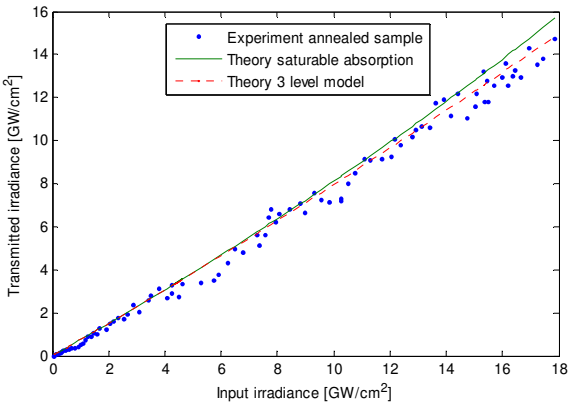

(a)

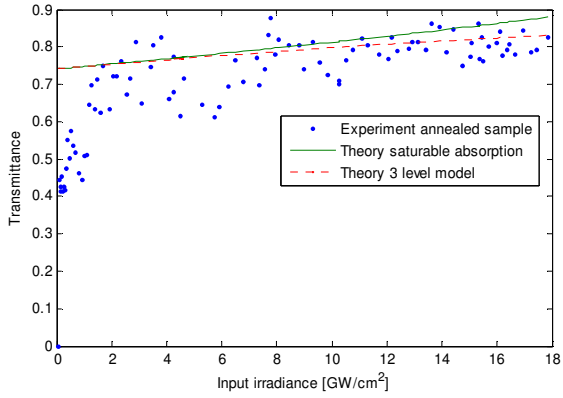

(b)

Fig. 7. Optical transmittance through the annealed sample (a) transmitted vs. incident irradiance, (b) transmittance as function of incident irradiance.

In agreement with our experiments, the annealing process generates an increment in the nc-Si size and density in the film, and also a modification of α_0 at this wavelength, due to a change in the resonance conditions of the material. The modification of the magnitude of the nonlinear response by means of an annealing process has been observed in other nanostructure materials [48]. At this point it is significant to say that we did not detect any important nonlinear optical absorption in a pure silicon-nitride sample. The complex dependence of the transmittance of our samples as a function of input irradiance observed in both Fig. 6b, and Fig. 7(b), points to a nonlinear absorption arising from ground and excited-state absorption. In order to investigate this dependence, we used a three-level model that has been previously applied to compounds that can present different mechanisms of nonlinear absorption [49]. This model predicts an irradiance dependent absorption coefficient $\alpha(I)$ given by:

#105953 - $15.00 USD Received 5 Jan 2009; revised 18 Mar 2009; accepted 25 Mar 2009; published 1 Jun 2009

$$\alpha(I) = \alpha_0 \left\{ \frac{1 + I/I_s[1 + \sigma_r(1 + \tau_r)]}{1 + (2 + \sigma_r \tau_r) I/I_s + 3\sigma_r \tau_r (I/I_s)^2} \right\}, \tag{11}$$

where $\alpha_0 = \sigma_{12} N_0$, with σ_{12} the absorption cross-section from the ground to the first excited state ($|1\rangle \rightarrow |2\rangle$); $\sigma_r = \sigma_{23}/\sigma_{12}$ is the ratio of excited- to ground-state absorption; $\tau_r = \tau_{32}/\tau_{21}$ is the corresponding lifetime ratio; and $I_s = \hbar\omega/\sigma_{12}\tau_{21}$ is the saturation irradiance. The model was used to fit the nonlinear absorption of both the annealed and the as-grown samples, Fig. 6 and Fig. 7 show the fit to the data of irradiance and transmittance obtained for the samples. We use the value I_s=3.40x10^{14} W/m^2 calculated previously for the annealed sample, and from the fit to the experimental data for the annealed sample we obtained σ_r=0.9, and τ_r =10. For the as-grown sample we obtained I_s=2.15x10^{15}W/m^2, σ_r=50 and τ_r =0.15. From these results we can observe that the best fit showed in Fig. 6 and Fig. 7 are obtained when the saturation irradiance and the lifetime ratio are different for the as-grown sample in comparison to the annealed sample; this is an expected result if we consider that the value of σ is different for each sample. We observe that the annealing process modifies strongly the linear absorption coefficient related with the number and size of nc-Si in the film. As a comparative result, we measured the nonlinear optical response in a similar silicon-nitride film with an average size of nc-Si of about 3.1±0.37 nm and a density of approximately of 2.15×10^{11} cm^{-2}. The nc-Si size of this third sample corresponds to a value near to the size of our as-grown sample and its density corresponds approximately to the nc-Si density of our annealed sample. Our experiments with 26 ps pulses at 532 nm indicate that for this case α_0=7.0093×10^5 m^{-1}, β=-1×10^{-9}m/W, n_2=2.2×10^{-16}m^2/W, and $\left|\chi^{(3)}_{1111}\right|$=2.75×10^{-10}esu.

This last sample has been studied in the nanosecond and femtosecond regime, and our results are in good agreement with the parameters previously reported for it [36]. Comparing the nonlinear parameters obtained, we observe that the value of n_2 increases as a function of the nc-Si density; while the opposite behavior is presented by the β value. Moreover, we show that it is not only possible to decrease the value of β by means of an increment of the nc-Si density; but it is even possible to change its sign, i.e. change from an induced to a saturable absorption regime. The reason for this sign change is the modification of the linear absorption as a consequence of the annealing process, changing considerably the resonance conditions, and hence the ratio of ground-to excited-state absorption cross sections. This control of the magnitude and sign of the nonlinear absorption coefficient by the annealing process is very interesting, since induced absorption is a deleterious effect for possible applications of these materials in optical signal processing devices. In principle we can refine the annealing process in order to make nonlinear absorption negligible, which can be important for developing materials with promising applications in all optical switching devices.

5. Conclusion

We report TPA and optical saturation at 532 nm with 26 ps pulses in silicon-nitride films containing nc-Si and prepared by RPECVD. The response time of the samples was estimated by measuring the nonlinear optical transmittance and the density of the nc-Si into the annealed sample. We consider a vectorial self-diffraction effect to identify an electronic response as the main physical mechanism responsible for the observed nonlinear refraction. This electronic response is due to quantum confinement effects. An annealing process in this kind of films prepared by RPECVD produces an enhanced PL signal. Because the annealing process also produces an increment in the density and size of the nc-Si into the film, the optical Kerr response is not enhanced; however, it is interesting to observe that nonlinear optical absorption can be modified from induced absorption to optical saturation, when the linear

#105953 - $15.00 USD Received 5 Jan 2009; revised 18 Mar 2009; accepted 25 Mar 2009; published 1 Jun 2009

optical absorption is changed by means of an increase of the size and density of nc-Si into the film. We used an input-output experiment for confirming the mechanism of nonlinear optical absorption in the nc-Si in the film. We also found that our samples exhibit a high ablation threshold.

Acknowledgments

The authors wish to acknowledge the technical assistance of K. López, F.J. Jaimes, L. Rendón and D. Quiterio-Vargas. This work has been partially supported by DGAPA-UNAM under projects PAPIIT-IN101908-2, PAPIIT-IN108807-3, by IPN under project SIP-20090138 and by CONACYT under projects 82708, 80019, 47303 and 46492, 48970.

#105953 - $15.00 USD Received 5 Jan 2009; revised 18 Mar 2009; accepted 25 Mar 2009; published 1 Jun 2009